coatings

MDPI

Article

Self-Healing Performance of Cellulose-Based Gel Coating with Highly Loaded Hybrid Inhibitor

Xiong Zhao [1], Jixing Wang [2], Haibing Zhang [3], Hailong Zhang [2,4], Lu Ma [1], Xianfeng Zhang [1], Wenhua Cheng [3], Huiyu Zhang [2], Ali Hussein Khalaf [2], Bing Lin [2,*] and Junlei Tang [2,*]

[1] Science and Technology Research Institute, China Three Gorges Corporation, Beijing 100038, China; ma_lu4@ctg.com.cn (L.M.)
[2] School of Chemistry and Chemical Engineering & Institute for Carbon Neutrality, Southwest Petroleum University, Chengdu 610500, China; jixing_wang02@yeah.net (J.W.); hailong0902@126.com (H.Z.)
[3] State Key Laboratory for Marine Corrosion and Protection, Luoyang Ship Material Research Institute, Qingdao 266237, China; chengwh@sunrui.net (W.C.)
[4] School of Materials Science and Engineering, Xihua University, Chengdu 610039, China
* Correspondence: h1900@foxmail.com (B.L.); tangjunlei@126.com (J.T.)

Abstract: The self-healing performance of an ethyl-cellulose-based gel coating with different corrosion inhibitors was investigated in this work. Various contents of 11 alkyl imidazoline (IMO-11) were pre-loaded into the gel coating. The EIS results of scratched coatings with inhibitors confirmed the self-healing performance of the coating. As the inhibitor contents increased, the improved self-healing effect was attributed to inhibitor release, while the increased inhibitor content would also affect the film-forming ability and mechanical properties of the composite coating, and lead to the accelerated failure of the coating. Different contents of thiourea and sodium oleate were added to the gel coating with 25% IMO-11. It was hoped that the hybrid inhibitor in the coating would obtain the synergistic effect of different inhibitors during the self-healing progress. The SEM and FT-IR results indicate the hybrid inhibitor was successfully loaded into the gel coating. The EIS and morphology results of scratched coatings confirmed the enhance effect of the synergistic inhibitor on the self-healing performance of the coating. The high content of the hybrid inhibitor could enhance the corrosion protection effect of the intact gel coating. Once the coating is damaged, the fast released inhibitor could extend the corrosion protection time. The synergistic effect difference of thiourea and sodium oleate with IMO-11 did not show much difference in the coating self-healing effect in this work.

Keywords: gel coating; self-healing performance; synergistic effect of inhibitor

Citation: Zhao, X.; Wang, J.; Zhang, H.; Zhang, H.; Ma, L.; Zhang, X.; Cheng, W.; Zhang, H.; Khalaf, A.H.; Lin, B.; et al. Self-Healing Performance of Cellulose-Based Gel Coating with Highly Loaded Hybrid Inhibitor. *Coatings* **2024**, *14*, 917. https://doi.org/10.3390/coatings14070917

Academic Editor: Olga A. Shilova

Received: 21 June 2024
Revised: 15 July 2024
Accepted: 19 July 2024
Published: 22 July 2024

1. Introduction

In recent years, self-healing coatings have received a lot of attention due to their ability of recover barrier properties upon damage [1]. Inspired by the skin self-repair phenomenon in bionics, researchers proposed the concept of self-healing coatings to extend the corrosion protection time. According to the different healing mechanisms, self-healing coatings can be classified as intrinsic and extrinsic coatings [1,2]. As a typical extrinsic self-healing strategy, adding corrosion inhibitors into coatings to achieve a self-healing effect is an important research direction.

In general, the method to load corrosion inhibitors into coatings is including direct addition [3], microcapsules [4], and nanofibers [5], etc. Many researchers focused on the direct addition of corrosion inhibitors into coatings, and concluded the influence of inhibitors on coatings' self-healing effect. The inhibitors should not react with the coating substrate, to make sure they can all play a part in corrosion protection. The total content of the inhibitor loaded in the coating could determine the self-healing effect and duration. Finally, the effective content of an inhibitor could release to the damaged area of the coating to achieve a self-healing effect. Unfortunately, the self-healing coatings based on corrosion

inhibitors usually have low inhibitor capacity. Therefore, the majority of studies find that self-healing coatings have great anti-corrosion performance in limited timeframes. There is still a long way to go before a self-healing coating is used in the industrial field. In our previous study, a gel coating based on a super molecular assembly effect is investigated [6,7]. Utilizing the large number of hydrogen bonds in this gel coating, an intrinsic healing method using magnetothermal properties was developed [8]. Nanocontainer encapsulated inhibitors were also added to the gel coating to achieve self-healing ability in a corrosion environment containing CO_2 and Cl^- [9]. In order to further understand the extrinsic self-healing effect of this kind of gel coating, imidazoline inhibitors with different carbon chains were used to introduce self-healing properties to the gel coating [10]. The imidazoline inhibitor dissolved in the three-dimensional network of the gel coating could release from the coating scratches to enhance the corrosion protection performance. Consequently, it is critical to enhance this sort of gel coating's ability to cure itself and its ability to prevent corrosion. Based on the 3D network of gel materials, organic inhibitors could pre-load into the gel material to enhance the anti-corrosion performance and self-healing effect of a gel [10]. The 3D network in the gel coating would also control the release rate of the inhibitor once the gel was damaged. Therefore, improving the adaptability of the inhibitors and gel coating structure plays a key factor in the development of this kind of coating. It is worth exploring further to enhance the self-healing effect of this kind of self-healing gel coating.

It is the simplest and most effective way to improve the corrosion inhibition efficiency by using the synergistic effect between different inhibitors to obtain a hybrid inhibitor. With a small dosage, hybrid corrosion inhibitors can achieve excellent inhibitory efficiency and lower use costs [11,12]. In comparison with the single type inhibitor, the adsorption film of the hybrid inhibitor would be denser. And the denser protection film could prevent the contact of aggressive ions and metals. The synergistic effect of an imidazoline inhibitor with other inhibitors has been thoroughly explored, as it is one of the most often used corrosion inhibitors in the industrial field. Zhu et al. [13] confirmed the synergistic effect of a mercaptoethanol (ME) inhibitor and oleate imidazoline (OIM). They revealed the optimal compounding ratio of the two inhibitors, and pointed out that ME could fill the void of the OIM film to achieve a denser adsorption film. Wang et al. [14] compared the synergistic effect between dithiothreitol (DTT) and ME with OIM. And the results revealed that DTT-OIM adsorption film has better stability and anti-corrosion performance for carbon steel in Cl^- solution with saturation CO_2. Ren et al. [15] investigated the inhibition effect of imidazolinyl asymmetric quaternary ammonium salts (DBA) and thiourea (TU). The hybrid inhibitor could inhibit the anode process of corrosion reactions, and the adsorption model conforms to the Flory–Huggins adsorption isotherm. And the synergistic effect of DBA and TU was most significant at the total content between 100 to 200 mg/L. Okafor et al. [16] studied the synergistic effect between sodium 2-undecyl-1-acetate-imidazoline salt (2M2) and TU. The relative content of two inhibitors could affect the inhibition efficiency, and the 2M2-TU adsorption film formed could prevent the corrosion reactions. A synergistic effect between inhibitors is a hotspot for corrosion protection research. And scholars are trying to load the hybrid inhibitor into coatings to achieve good self-healing properties. Mohammadloo et al. [17] prepared a urealdehyde microcapsule loaded with cerium acetate (Ce-a) and 8-hydrocyquinoline (8-HQ). By adding the microcapsule to the epoxy coating, better anti-corrosion performance and active anti-corrosion properties are obtained in comparison with a pure epoxy coating. Sanaei et al. [18] revealed organic and inorganic hybrid inhibitors could enhance the self-healing performance of anti-corrosion coatings, particularly in extending the protection time after the coating was damaged. Therefore, the hybrid inhibitor with synergistic effect could enhance the anti-corrosion performance of self-healing coatings [19]. And it is necessary to further research the synergistic inhibition effect between inhibitors in self-healing supramolecular gel coatings.

To further develop the corrosion protection technology based on supramolecular gel material, and enhance the anti-corrosion performance and self-healing property of gel

coatings, in this work, an ethyl-cellulose-based gel coating with various contents (25%~33%) of 11 alkyl imidazoline (IMO-11) was prepared to investigate the influence of inhibitor on the self-healing effect of the gel coating. Thiourea and sodium oleate were added into the gel coating with 25% IMO-11 inhibitor. SEM and FT-IR were employed to study the structure characteristics of the gel coating. EIS and surface observation were used to understand the self-healing performance of gel coatings with hybrid inhibitors. This work is important to further increase the inhibitor content in the self-healing coating. And this novel coating could be used for the corrosion protection of flange and valve connections in pipelines, bolting connections in various industrial corrosive mediums, especially in the marine environment.

2. Experimental Details

2.1. Materials

Amounts of 11 alkyl imidazoline, thiourea, and sodium oleate were used as corrosion inhibitors to pre-load in gel coating. The inhibitors were provided (by Shanghai Aladding Biochemical Technology Co., Ltd., Shanghai, China), and the chemical structure of inhibitors is presented in Figure 1. Ethyl cellulose (EC), castor oil, and nano-TiO_2 are the main agents for the gel coating. O-xylene and anhydrous ethanol are the solvents of the coating. All chemical agents were unprocessed chemically pure reagents. The chemicals for gel coating preparation were supplied (by Chengdu Kelong Chemical Reagent Company, Chengdu, China), and there was no pre-processing for any chemicals before use.

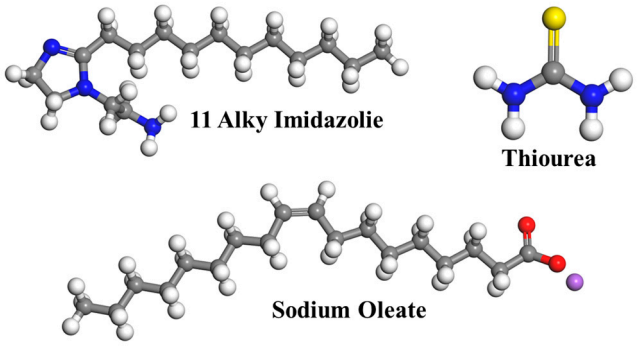

Figure 1. The chemical structure of test inhibitors.

A 20# steel coupon (provided by Taiyuan Iron & Steel Group Co., Ltd., Taiyuan, China) with a size of 40 mm × 15 mm × 2 mm was used as substrate to prepare coating samples. The chemical composite of 20# steel is C 0.2 wt%, Si 0.44 wt%, Mn 0.5 wt%, P 0.03 wt%, S 0.02 wt%, Cr 0.05 wt%, Ni 0.28 wt%, and the rest is Fe. Before being coated with gel coating, the steel coupons were polished to 1000# grit papers, washed with ethanol and deionized water, and then dried with cold air.

2.2. Preparation of Gel Coating with Inhibitors

Using a hot-melt blending process, 0.5 g TiO_2, 10.0 g castor oil, and 10.0 g ethyl cellulose were combined to form gel material. All the ingredients for the gel coating material were mixed and heated with stirring at 170 °C until the ingredients melted completely. The mixed solution was cooled down at room temperature to obtain the ethyl-cellulose-based gel coating material. Oxylene and anhydrous ethanol with a volume ratio of 5:1 were used as gel coating solvents. An amount of 10.0 g of gel material was dissolved in 300 mL of coating solvent. A specific amount of inhibitor was added to the coating solution and it was heated to 65 °C until the inhibitor dissolved completely. To test the tensile strength of the coating, the coating material was solidified into a column shape with diameter of 7 mm according to the GB/T 5210 standard [20] of China. A universal testing machine (GNT100, NCS Testing Technology Co., Ltd., Beijing, China) was employed to measure the tensile

strength with a 0.5 mm/s extension rate; 3 parallel samples were tested for each condition and the average value is listed in Table 1.

Table 1. Mechanical and adhesive characteristics of prepared coatings.

Coating Type	Tensile Strength (MPa)	Adhesive Force (MPa)
EC coating	1.86 ± 0.03	1.24 ± 0.02
EC coating with 25% IMO-11	1.54 ± 0.08	1.07 ± 0.04
EC coating with 25% IMO-11+6.25% Thiourea	1.45 ± 0.06	1.06 ± 0.04
EC coating with 25% IMO-11+12.5% Thiourea	1.32 ± 0.11	1.01 ± 0.03
EC coating with 25% IMO-11+6.25% Sodium Oleate	1.47 ± 0.05	1.02 ± 0.05
EC coating with 25% IMO-11+12.5% Sodium Oleate	1.28 ± 0.09	0.94 ± 0.02

On 20# steel, the coating was applied with a brush at room temperature. An eddy current thickness meter was employed to measure the thickness of the prepared coating. And the thickness for all coatings prepared in this study was about 300 ± 10 μm. The adhesive force between gel coating and steel was measured by a DeFelsko Positest AT-A pull-out adhesion tester (DeFelsko Corporation, Ogdensburg, NY, USA). For each coating, 5 parallel samples were tested and the average value is listed in Table 1.

2.3. Anti-Corrosion Performance of the Prepared Coatings

2.3.1. Electrochemical Impedance Spectroscopy (EIS) Measurement

In order to understand the self-healing performance of the gel coating with inhibitor, a 10 mm length artificial scratch was made by a knife on the coating, which is deep to substrate steel. EIS was employed to study the anti-corrosion behavior and self-healing performance of prepared coatings by an electrochemical workstation (CS 350, Wuhan Corrtest Instruments Corp., Ltd., Wuhan, China).

A three-electrode system was used in the EIS test. Saturated calomel electrode (SEC) served as the reference electrode, prepared coatings served as the working electrode, and platinum served as the counter electrode. Open circuit potential (OCP) monitoring for 15 min was performed first. Subsequently, an EIS test was conducted at OCP using a scanning frequency range of 100 kHz–0.01 Hz and a potential perturbation of 15 mV. Furthermore, ZSimpWin V3.0 software (v3.0) (AMETEK Scientific Instruments, Berwyn, PA, USA) was used to fit the EIS results. In this study, room temperature, saturated CO_2 in a 3.5 weight percent NaCl solution served as the corrosion medium. Three experiments in parallel were conducted for each type of coating.

2.3.2. Inhibitor Releasing Test

Ultraviolet and visible spectrophotometry (UV–vis, UV-1800PC, AOELAB, Shanghai, China), was employed to determine the release behavior of the imidazoline inhibitors from gel coating in corrosion medium. Release profiles were acquired by plotting the absorbance of imidazoline in corrosion solution at the wave length of 210 nm as a function of the time.

2.3.3. Surface Characterization

The cross-section and surface morphology of the gel coating were observed using scanning electron microscopy (SEM, S-4100, Hitachi, Tokyo, Japan). Magnifications of 150 and 1000 times were used to observe the cross-section of prepared gel coating with various inhibitors. Optical microscope (Axio Zoom, V16, ZEISS, Oberkochen, Germay) combined with SEM (magnify 120 times) were used to observe the corrosion morphology of scratched area on the gel coating with various inhibitors.

The chemical characteristics of the gel coating with inhibitor were investigated using an FT-IR Fourier transform infrared spectrometer (FT-IR, WQF-520, Beifen-Ruili, Beijing, China). The spectra were recorded in the range of 4000–500 cm^{-1} 64 times.

3. Results and Discussion

3.1. Effect of IMO-11 Inhibitor Content on the Gel Coating Self-Healing Behavior

In our previous study [10], synthesized imidazoline inhibitors with different length carbon chains were pre-loaded into the ethyl-cellulose gel coating. The enhanced effect of inhibitors on anti-corrosion performance and self-healing effect has been proven. To further investigate the effect of inhibitor content on gel coating corrosion protection, a series ethyl-cellulose gel coatings with various IMO-11 inhibitors was prepared on Q235 carbon steel. A 10 mm artificial scratch penetrating the steel was made on the coating sample. Figure 2 displays the electrochemical impedance spectroscopy (EIS) results of prepared samples that were submerged in a 3.5 weight percent NaCl solution with saturated CO_2 for different periods of time. The EIS test was measured on the 1st, 3rd, 7th, 10th, and 15th days to investigate the anti-corrosion performance of coatings.

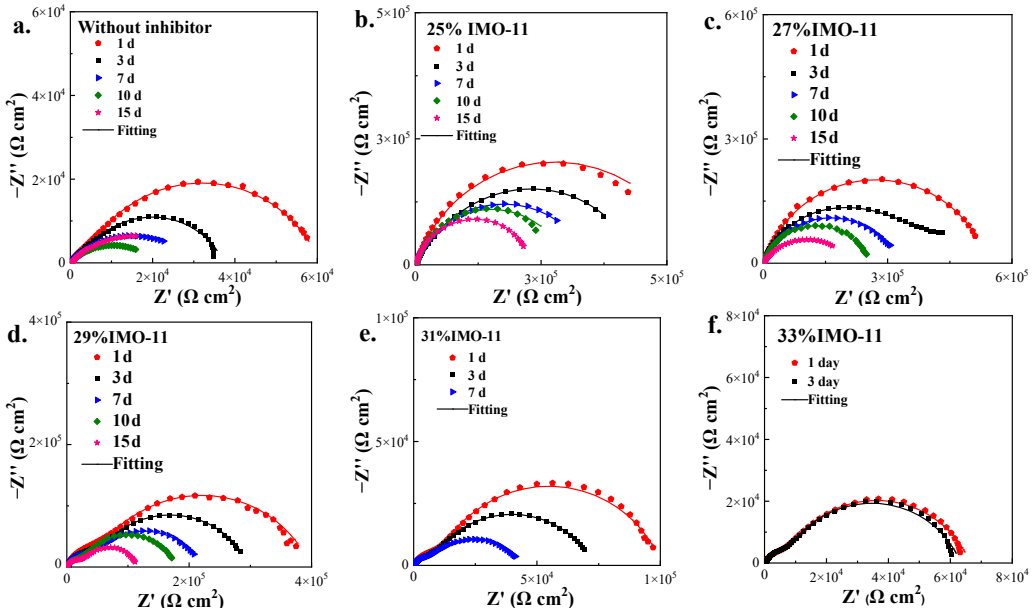

Figure 2. Nyquist plots of artificial scratched gel coating with various contents of IMO-11 inhibitor immersed in test solution for different periods: (**a**) without; (**b**) 25%; (**c**) 27%; (**d**) 29%; (**e**) 31%; (**f**) 33%.

As shown in Figure 2, the Nyquist plots of ethyl-cellulose gel coating with various contents of IMO-11 inhibitor all showed a single capacitive loop, indicating the good corrosion protection effect of the damaged coating [21,22]. As the immersion time increased for each inhibitor content coating, the capacitive loop's radius decreased. When compared to a coating without an inhibitor, the rate of decrease was substantially slower. This outcome demonstrated the self-healing effect of the gel coating with inhibitor, which is consistent with the previous work [10]. Moreover, as the inhibitor content increased, the capacitive loop radius slightly decreased. And the radius of the capacitive loop of gel coating without inhibitor and with 33% IMO-11 are almost the same, which is mainly attributed to the prototyping ability and adhesive force of the gel coating. The ethyl-cellulose-based gel coating investigated in this work has a 3D network structure. Cross-linked cellulose molecules act as the polymer matrix, and the small-molecule oil acts as the dispersed phase [23]. The intact gel coating would physically isolate the corrosive medium from the metal substrate, and the added inhibitor would enhance the corrosion protection effect [9,10]. For the scratched coating, the fast release of the inhibitor from the coating could suppress the corrosion reactions by forming an adsorption inhibitor film at the

scratched area, leading to the impedance value of the gel coating with inhibitor being higher than that of the coating without inhibitor. On the other hand, the release of the inhibitor would lead to the reduction in the dispersed phase in the gel coating structure, especially for the coating with a high inhibitor content. In addition, the release of the inhibitor from the gel coating would also create a decrease in the adhesive force. The degradation of the coating structure and the decrease in the adhesive force could both lead to a significant decrease in the capacitive loop radius of EIS plots. And this is why there are only 7 days' results for the coating with the 31% inhibitor and 3 days' results for the coating with the 33% inhibitor.

Figure 3a summarizes the variation in $|Z|_{0.01\ Hz}$ of the prepared gel coating with different inhibitor contents in the test corrosion environment. $|Z|_{0.01\ Hz}$ could clearly reflect the variation in the corrosion protection performance of the scratched coating [10,21,22]. For the first immersion day, the $|Z|_{0.01\ Hz}$ values of the gel coating with 25%~29% inhibitor are quite close, at over $4 \times 10^5\ \Omega\ cm^2$. For the coating with 31% and 33% inhibitor, after 1 day of immersion, the $|Z|_{0.01\ Hz}$ value is less than $10^5\ \Omega\ cm^2$, which is only slightly higher than that of the coating without inhibitor. This result reveals that excessive content of the inhibitors will decrease the film-forming ability of the gel coating [10] and decrease the corrosion protection effect. As the immersion time increases, the $|Z|_{0.01\ Hz}$ decreases. For all conditions, the $|Z|_{0.01\ Hz}$ value is significantly higher than the coating without inhibitor, strongly indicating the great self-healing performance of the gel coating with inhibitor. The inhibitor could release at the scratched area of the coating and be adsorbed on the steel substrate to form an anti-corrosion film. As a result, there is a clear correlation between the inhibitor release rate and amount and the gel coating's self-healing ability.

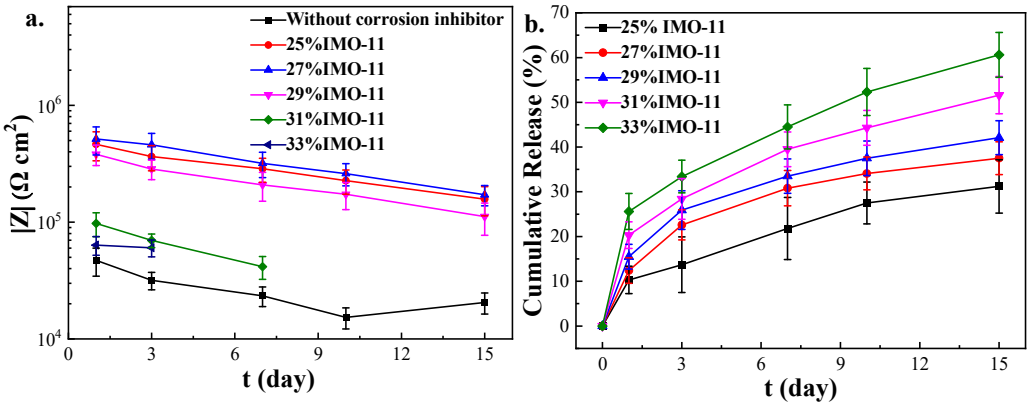

Figure 3. (**a**). Summarized $|Z|_{0.01\ Hz}$ value of EIS results in Figure 2; (**b**) cumulative release of IMO-11 inhibitor from gel coating.

The cumulative release rate of gel coatings with different IMO inhibitor contents was measured by UV–visible spectrophotometry [24,25], and the results are presented in Figure 3b. For the first immersion day, the cumulative release ratio of the gel coating with 25% to 33% IMO inhibitor is 10.3%, 12.4%, 15.5%, 20.3%, and 25.6%, respectively. This result reveals that the inhibitor release amount increased as the pre-loaded content increased. For the gel coating with a high content inhibitor, the inhibitor would be easily released into the corrosion medium. Inhibitors act as part of the dispersed phase of the gel structure; lots of inhibitors do not interact with the gel skeleton structure, which could rapidly migrate to the corrosive medium. As the immersion time increased, the total cumulative release ratio of the inhibitor gradually increased. After 15 days of immersion, the largest release ratio decreased as the inhibitor content in the gel coating decreased. As discussed above, the physical barrier effect of the coating would be decreased by an excessively large release amount of the inhibitor. Therefore, the appropriate content of inhibitor loaded into the gel coating is a key factor for engineering applications. In an

atmospheric corrosive environment, a gel coating with ultrahigh inhibitor content could provide a great barrier effect and rapid self-healing effect to protect the metal substrate.

3.2. Character of Supramolecular Gel Coating with Hybrid Inhibitors

According to the EIS results of scratched gel coating with various inhibitor contents, the fast release of the inhibitor in an aqueous corrosion medium would lead to a decrease in adhesive force and shorten the service time. To avoid the influence of corrosion inhibitors in the gel coating, the following research was carried out for the gel coating with a 25% IMO-11 inhibitor. Based on the formulation of gel coating with a 25% inhibitor, thiourea and sodium oleate were added to the gel coating, to further investigate the synergistic effect of inhibitors on gel coating. Figure 4 shows the cross-section of the gel coating with different ratios of hybrid inhibitors. And the gel coating without inhibitor and with a 25% IMO-11 inhibitor are also presented.

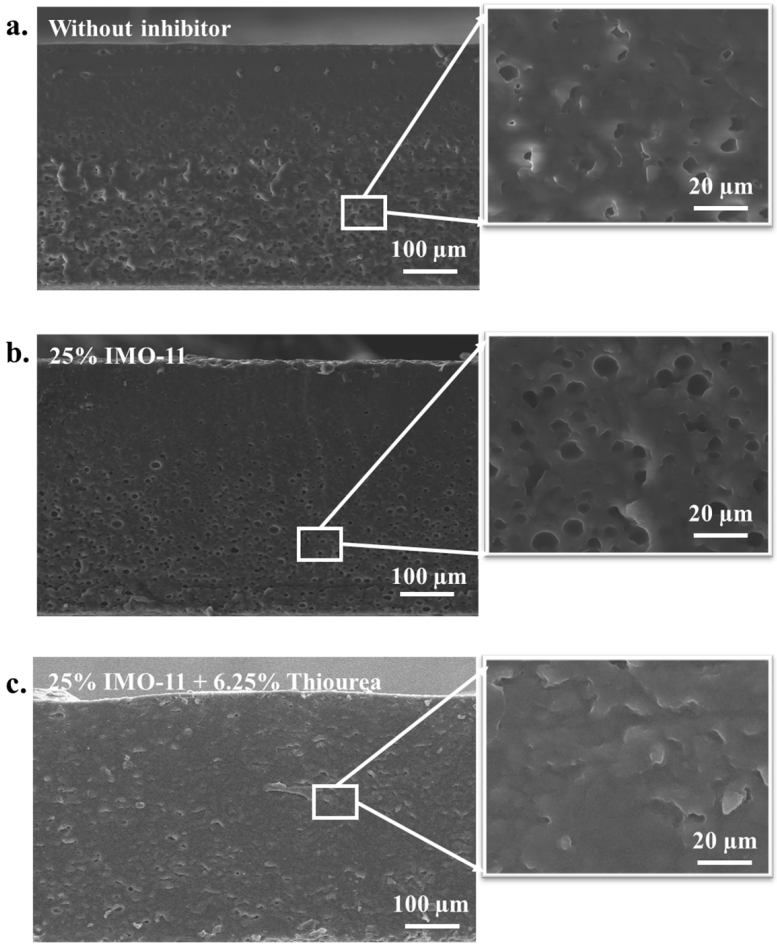

Figure 4. *Cont.*

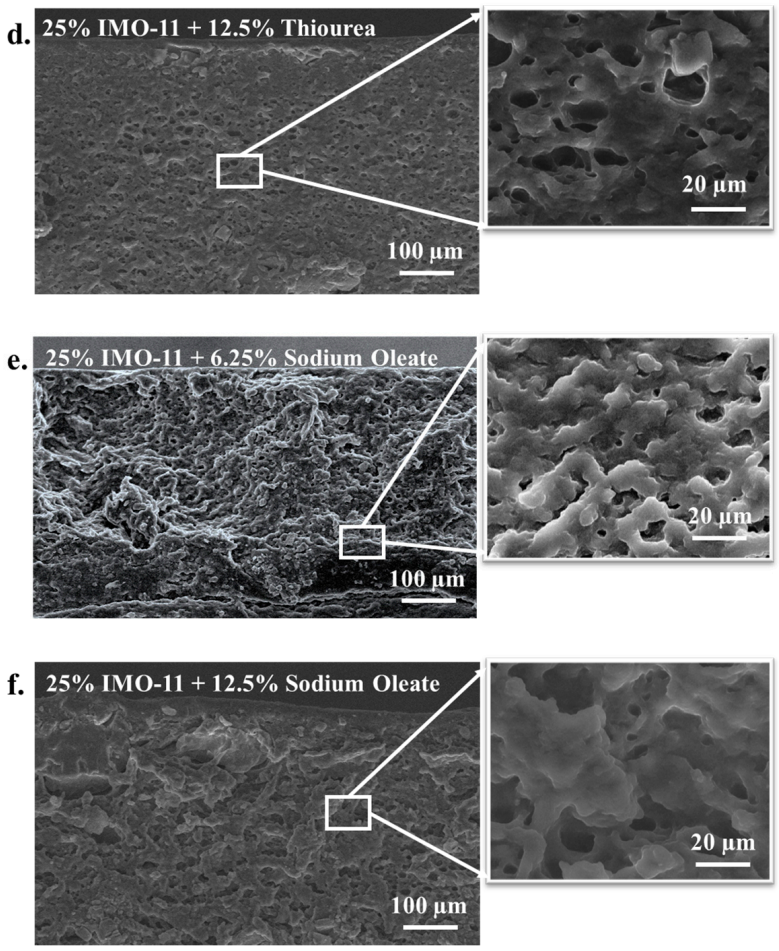

Figure 4. Cross-section morphology of gel coating with various kind of inhibitors: (**a**) without inhibitor; (**b**) 25% IMO-11; (**c**) 25% IMO-11 and 6.25% thiourea; (**d**) 25% IMO-11 and 12.5% thiourea; (**e**) 25% IMO-11 and 6.25% sodium oleate; (**f**) 25% IMO-11 and 12.5% sodium oleate.

There are several "honeycomb"-shaped cavities in the coating's cross-section for the inhibitor-free coating (Figure 4a). The gel coating without inhibitor is formed by the ethyl-cellulose skeleton structure and the dispersed phase of the small-molecule oily substance (castor oil in this research). The cavities are the dispersed phase in the gel coating, which lead to the gel coating being able to hold a higher content of the inhibitor and have an effect on the filming performance and anti-corrosion performance of the coating [7–10]. After adding inhibitors to the gel coating (Figure 4b–f), the main structural features have not significantly changed. Only the size and density of cavities have changed. For the coating with inhibitor, the inhibitors and castor oil both act as dispersed phases in the gel structure. Parts of the inhibitor would have a cross-linking reaction with the ethyl-cellulose skeleton structure, which would enhance the stability of the gel coating and lead to improvement in the anti-corrosion performance. The remaining inhibitor components are evenly distributed throughout the gel coating as a free dispersion phase. Once the coating is damaged, the free inhibitor could rapidly release into the corrosion medium and form an anti-corrosion adsorption film on the metal substrate. And the high content of inhibitor could lead to the continuous release of the inhibitor from the coating to provide a longer corrosion protection effect [26,27]. In addition, according to results of this section, the hybrid inhibitor of IMO-11 with thiourea or sodium oleate has no obvious difference.

Figure 5 displays the ATR FT-IR results of the gel coating made of ethyl cellulose both with and without various inhibitors. Figure 5a shows the spectra for the gel coating without inhibitor and with 25% IMO-11. The absorption peak at 1061 cm^{-1} is attributed to the stretching vibration of the C-O-C bond in ethyl cellulose and castor oil [10,28,29].

The peaks at 1378 cm^{-1}, 1446 cm^{-1}, and 1741 cm^{-1} represent the C=C [28], C-O [29], and C=O [28,29] bonds in the gel coating, respectively. The absorption peaks at 2927 cm^{-1} and 2858 cm^{-1} are the asymmetric and symmetric stretching vibration peaks of -CH_3 and –CH_2- in the cellulose molecular, respectively [10,30]. And the broad peak at 3476 cm^{-1} is associated with the hydrogen bonds in the gel coating. For the gel coating with IMO-11, the characteristic peaks at 1553 cm^{-1} and 1635 cm^{-1} represent the imidazole ring and C=N bond, respectively. The FT-IR results confirmed the IMO-11 inhibitor and castor oil act as dispersion phases in the gel coating. And the inhibitor mainly exists in the coating through physical dissolution and hydrogen bonding. The FT-IR results for the gel coating with the hybrid inhibitors are shown in Figure 5b,c. There is almost no difference in the fingerprint peaks of the gel coating with hybrid inhibitors or with IMO-11 inhibitors alone. This phenomenon is mainly due to the similarity of the characteristic peaks of thiourea [31] and sodium oleate [32] withIMO-11. Therefore, the addition of thiourea or sodium oleate alone only can affect the intensity of the characteristic peaks. In addition, there is no new bonding form after the hybrid inhibitor is loaded into the gel coating, indicating the hybrid inhibitor was added to the gel coating via physical dissolution and hydrogen bonding. And this result could guarantee the fast release of inhibitors into the corrosion medium to suppress corrosion reactions once the coating is damaged.

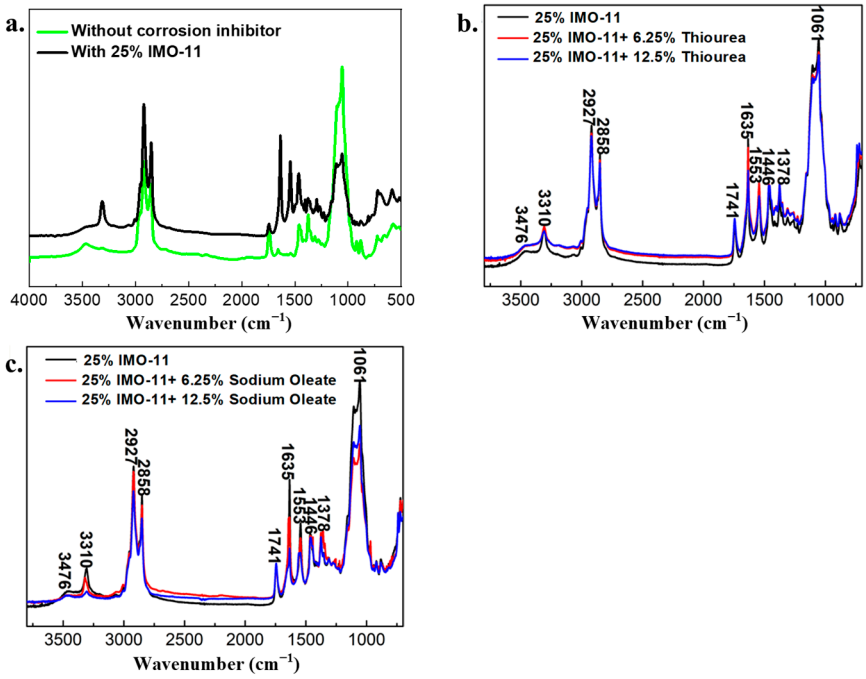

Figure 5. FT-IR spectra of gel coating without and with different inhibitors; (**a**) without and with 25% IMO-11; (**b**) with IMO-11 and thiourea; (**c**) with IMO-11 and sodium oleate.

3.3. Self-Healing Performance of Gel Coating with Hybrid Corrosion Inhibitor

EIS measurement was performed on the artificial scratched gel coating with different hybrid inhibitors (IMO-11 and thiourea, or IMO-11 and sodium oleate) and different inhibitor ratios (4:1 or 2:1) in 3.5 wt% NaCl solution with saturated CO_2, and the Nyquist and Bode plots are presented in Figure 6. The EIS results for the gel coating with the hybrid inhibitor are little different from those of the coating only loaded with IMO-11 in Figure 2. Shown in the Nyquist plots (Figure 6a,c,e,g) is a semicircle indicating the corrosion performance of the self-healing effect [21]. For each condition, as the immersion time increased, the radius of the semicircle decreased. As shown in the Bode plots (Figure 6b,d,f,h), the phase angle of most conditions presents a peak at about 1 Hz. A broad "hump"-shaped peak that appears in only a few coating spectra containing 25% IMO-11 and 6.25% other inhibitor may be related to the inhibitor release behavior. As the test frequency dropped, the

|Z| value increased. Additionally, the behavior of the $|Z|_{0.01\ Hz}$ value changed similarly to the capacitive loop's radius in the Nyquist plots. Furthermore, the different types of hybrid inhibitors have no obvious effect on the self-healing effect of the gel coating. For the coating with 25% IMO-11 and 6.25% other inhibitor, the low ratio of the other kind of inhibitor limited the release amount of it. And the release of IMO-11 played a key role in the self-healing performance, and the release of thiourea or sodium oleate would slightly enhance the anti-corrosion performance due to the synergistic effect between inhibitors. The coating had a better self-healing effect when it contained 25% IMO-11 and 12.5% other inhibitor. The high amount of hybrid inhibitor in the gel coating could sustain release into the corrosive medium at the scratched area [10], and a dense compact absorption film could suppress the corrosion reactions. The equivalent circuit as shown in Figure 7 could be used to fit the EIS results for the scratched gel coating with various hybrid inhibitors, where R_s is the solution resistance, R_{ct} is the charge-transfer resistance, and R_{pore} represents the resistance at the coating damage area. CPE_{dl} and CPE_{coat} represent the capacitance of the electric double-layer and gel coatings. The fitted parameters are shown in Figure 8.

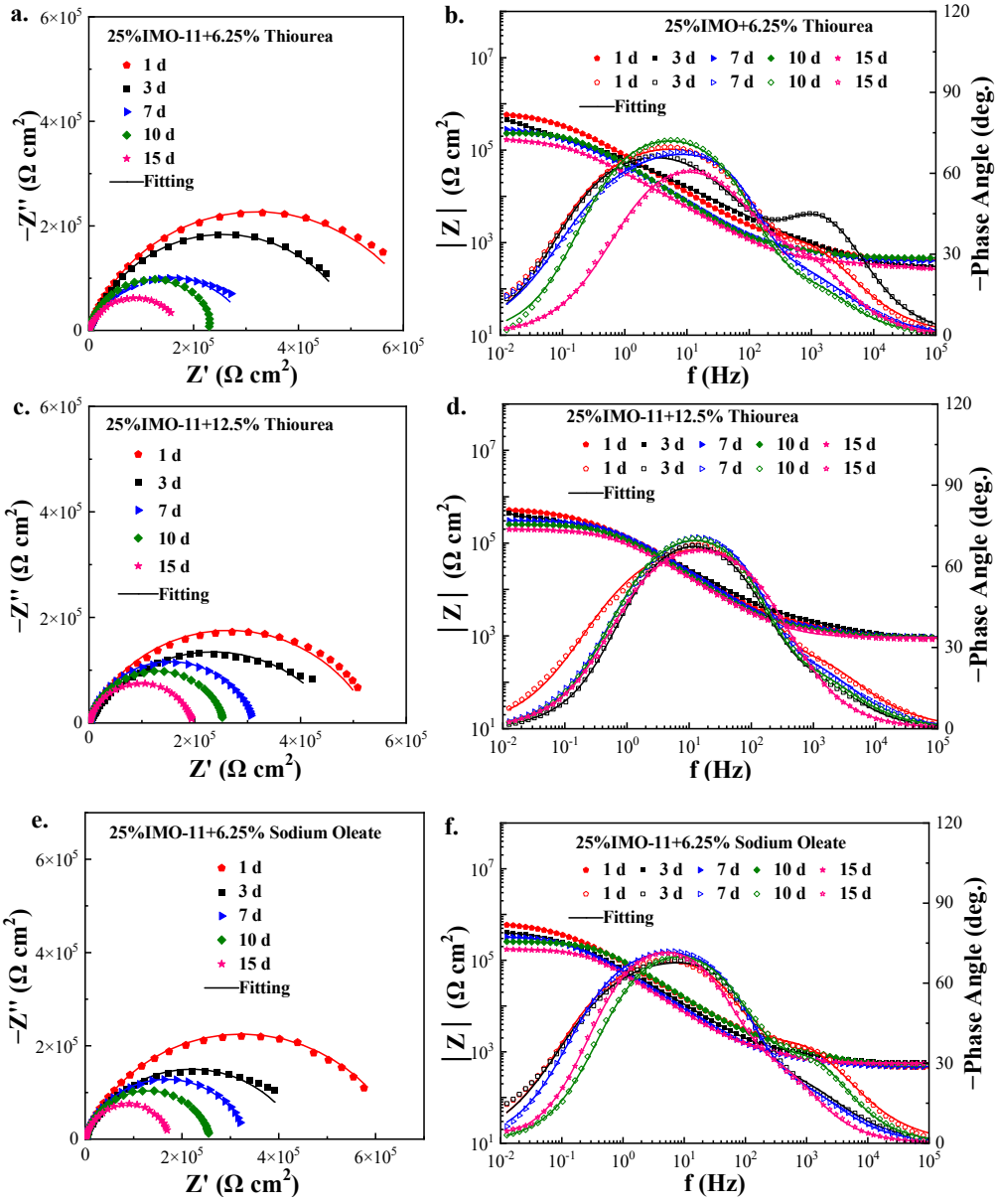

Figure 6. *Cont.*

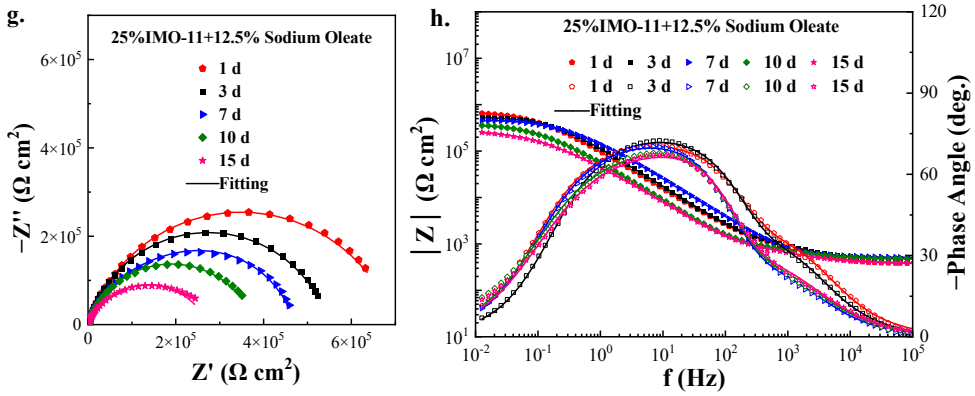

Figure 6. Nyquist and Bode plots of gel coating with hybrid inhibitors: (**a**,**b**) 25% IMO-11 and 6.25% thiourea; (**c**,**d**) 25% IMO-11 and 12.5% thiourea; (**e**,**f**) 25% IMO-11 and 6.25% sodium oleate; (**g**,**h**) 25% IMO-11 and 12.5% sodium oleate.

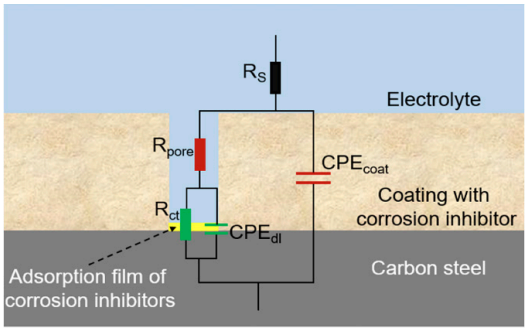

Figure 7. Equivalent circuit used to fit the EIS results in Figure 6.

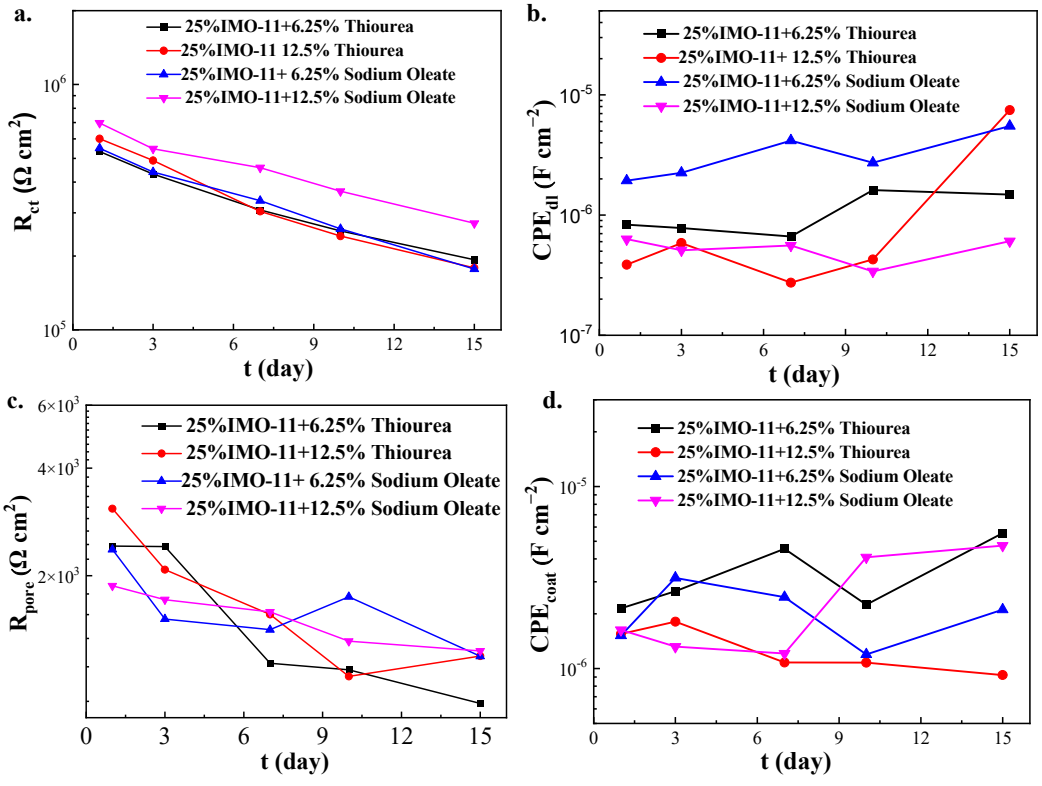

Figure 8. Electrochemical parameters fitted from the EIS results. (**a**) R_{ct}; (**b**) CPE_{dl}; (**c**) R_{pore}; (**d**) CPE_{coat}.

Figure 8a shows the fitted R_{ct} variation of the gel coating with the hybrid inhibitor. R_{ct} could directly reflect the self-healing performance of the coating with inhibitors [33]. For all test conditions, the R_{ct} value decreases as the immersion time increases, indicating the continuous degradation of the scratched coating in the corrosive medium. While the R_{ct} value decreased from about 7×10^5 Ω cm^2 to 2×10^5 Ω cm^2, this result revealed the self-healing performance of the gel coating with inhibitors. The coating with 25% IMO-11 and 12.5% sodium oleate showed the best self-healing performance for all conditions. On one hand, coatings with a higher content of inhibitor would show an enhanced self-healing effect [10]. The high inhibitor content could improve the instantaneous release amount due to the high ratio at the damage area [34]. Meanwhile, the high inhibitor content could extend the duration of the continued release behavior. On the other hand, the difference between the different inhibitor dissolution characteristics would affect the release behavior of the self-healing coating [35]. Thiourea is a water-soluble inhibitor, while sodium oleate has better solubility in oil. In the early stages of coating failure, a water-soluble inhibitor would rapidly release into an aqueous corrosive medium to protect the substrate, while the fast release of inhibitors without control would lead to a decrease in the continued release and durability of the coating. The oil-soluble inhibitor has a more moderate release rate, which leads to the best self-healing performance of gel coatings containing a synergistic inhibitor with 25% IMO-11 and 12.5% sodium oleate. Figure 8b shows the variation in the CPE_{dl}, which slightly increased as the immersion time increased. This result is due to the adsorption of the released inhibitor at the scratched area. The adsorption film formed by the inhibitor has a lower dielectric constant [36], which acts as a barrier effect to protect the steel surface. Figure 8c presents the variation in the R_{pore} value for the tested coatings during different immersion times. R_{pore} reflects the accumulation situation of corrosion products at the scratched area. And the corrosion products would affect the adsorption of inhibitors and the mass transfer of corrosion reactions. As shown in Figure 8d, the CPE_{coat} had almost no change during the 15 days' immersion, which suggests the great density and barrier effect of the gel coating with inhibitors. The good corrosion protection and self-healing effects of test coatings are mainly attributed to the pre-loaded inhibitors. The inhibitor could enhance the density and stability of the gel coating to enhance the barrier effect and prevent corrosion reactions. Additionally, the coating would have a self-healing effect due to the inhibitor's releasing characteristic. And, for this work, there is little difference in the self-healing performance between different synergistic inhibitor types. IMO-11, as the main inhibitor, has played a decisive role. And the thiourea and sodium oleate with different dissolution characteristics would affect the inhibitor release behavior and form a more stable adsorption film to enhance the self-healing performance of the gel coating.

The optical microscope and SEM were employed to observe the corrosion morphology of the scratched area of the gel coating with various inhibitors after 15 days of immersion. And the surface morphology of the immersed gel coating without inhibitor was observed. Numerous corrosion products are present at the scratched area of the gel coating without inhibitor, as seen in Figure 9a. The corrosion would occur at the damaged area of the coating and lead to the failure of the coating. For the coating with 25% IMO-11 (Figure 9b), the corrosion at the scratched area was significantly reduced due to the self-healing effect of the gel coating. The inhibitor released from the coating would form an adsorption film to protect the steel at the scratched area. For the coating with hybrid inhibitors (Figure 9c,d,e,f), almost no corrosion products can be found at the scratched area. These results further confirmed the great self-healing performance and corrosion protection effect of the released inhibitors from the gel coating.

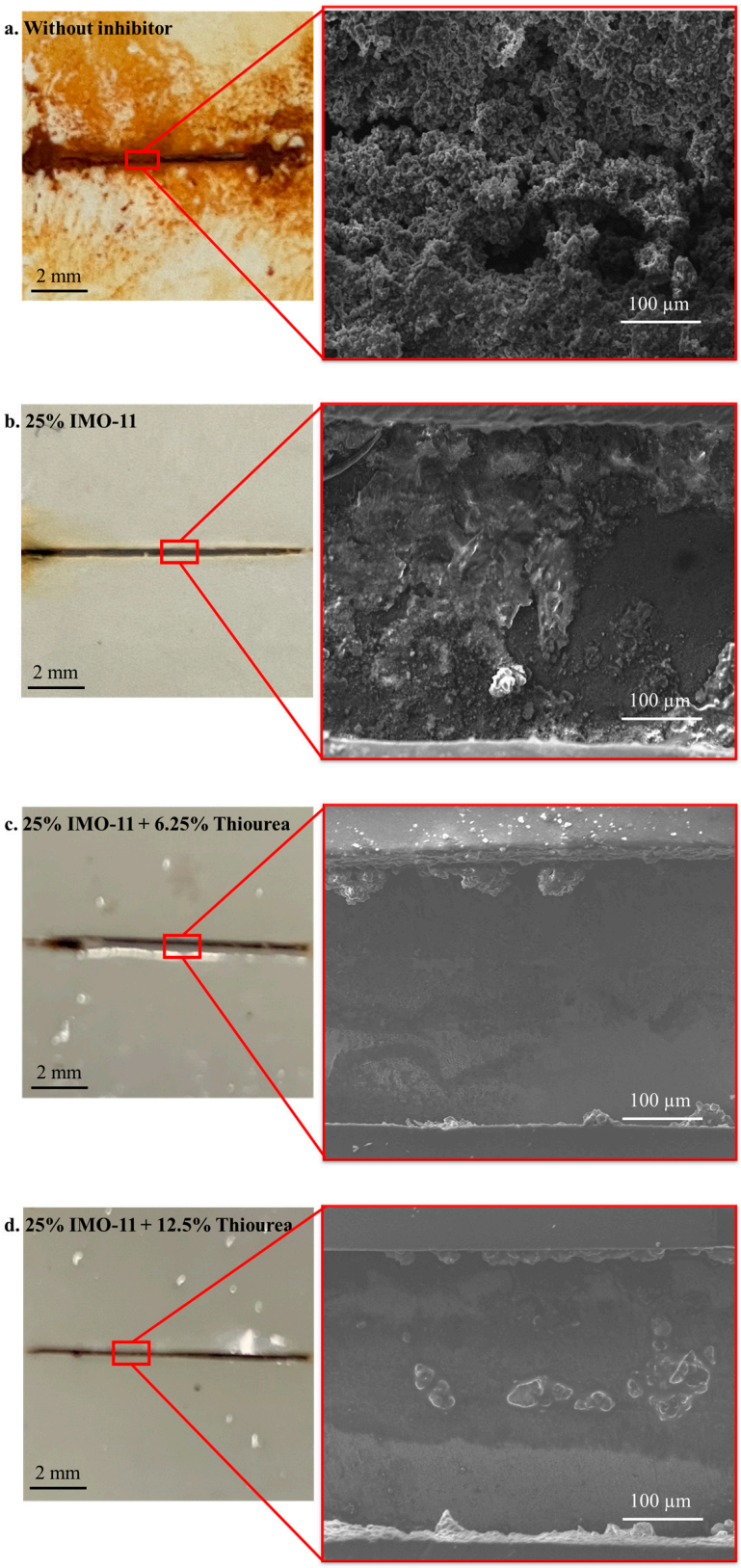

Figure 9. *Cont.*

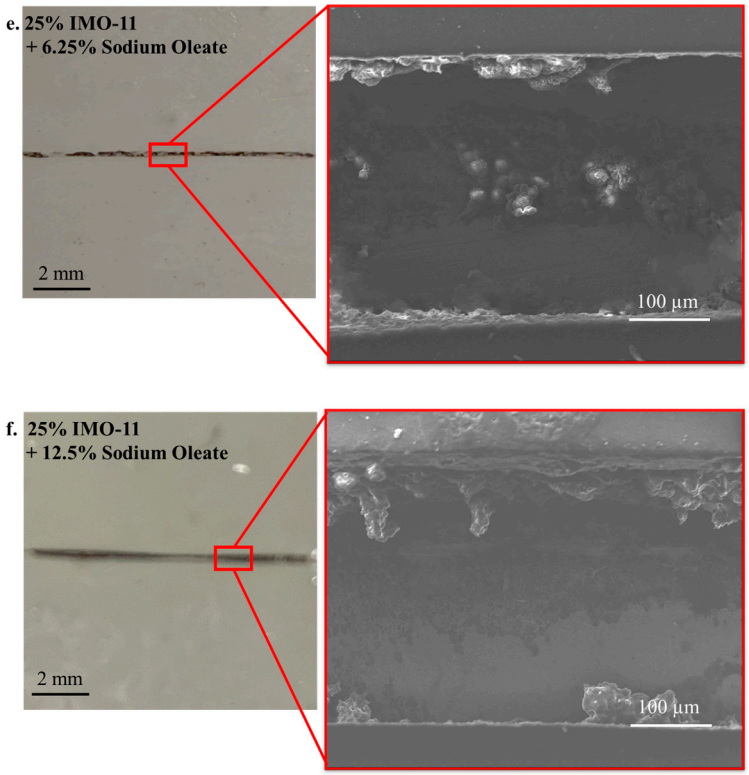

Figure 9. Surface morphology of scratched area on gel coating after immersed in test corrosion medium for 15 days. (**a**) without inhibitor; (**b**) 25% IMO-11; (**c**) 25% IMO-11 and 6.25% Thiourea; (**d**) 25% IMO-11 and 12.5% Thiourea; (**e**) 25% IMO-11 and 6.25% Sodium Oleate; (**f**) 25% IMO-11 and 12.5% Sodium Oleate.

3.4. Self-Healing Mechanism of Gel Coating with Hybrid Inhibitor

For intact gel coating, corrosion inhibitors are uniformly dispersed in the coating via physical dissolution and hydrogen bonding. The increased bonding density due to the addition of the inhibitor would improve the barrier effect of coating, which could separate the steel substrate and corrosive medium.

Once the gel coating with the inhibitor is damaged, the corrosion inhibitor will rapidly release into the aqueous corrosive medium. The released inhibitor could adsorb on the steel substrate, and the dense adsorption film could further protect steel from corrosion reactions. Simultaneously, the continuous releasing effect leading to a high inhibitor content at the affected location may encourage a more complete and denser inhibitor film. The inhibitor content pre-loaded in the gel coating would significantly affect the self-healing behavior. The highly loaded inhibitor would enhance the self-healing performance of the gel coating, while it would also decrease the film-forming ability and durability of the coating. In this research system, the inhibitor content of IMO-11 should not exceed 30%. As the immersion time of the damaged coating increased, the release rate of the inhibitor decreased. The inhibitor in the coating far from the damage area would migrate through the three-dimensional cavities in the gel coating. When the release rate is slower than the rate of the inhibitor diffusing into an aqueous corrosive medium, the impedance of the damaged area shows an obvious drop. Therefore, the long-term immersion of the damaged coating would decrease the self-healing performance. The high inhibitor content in the gel coating with the hybrid corrosion inhibitor ensured a good self-healing effect. The different solubleness of the inhibitor in the aqueous solution led to the different release rate of the hybrid inhibitor. In Section 3.3, the delayed release rate of sodium oleate yields the best self-healing effect when compared to thiourea. After long-term immersion, the adsorption film formed on the steel substrate at the damage area was a composite film. The synergistic effect between imidazoline and thiourea or sodium oleate would enhance the

anti-corrosion performance. And the self-healing performance of gel coatings containing inhibitors depends on the inhibition effect and mechanism of the inhibitor.

4. Conclusions

The ethyl-cellulose-based gel coatings developed in this work had different contents of 11 alkyl imidazoline, which significantly influenced the film-forming ability and self-healing performance. The addition of an inhibitor to the gel coating would increase the impedance of the coating, which would improve the corrosion protection effect of the gel coating. However, when the inhibitor content is over 30%, the film-forming ability and stability of the gel coating will decrease. Based on the EIS results and the cumulative release behavior of the artificially scratched coating, the gel coating with a 25%–29% inhibitor has excellent self-healing performance. The rapid, continuing release of the inhibitor could protect the steel in a scratched area from corrosion reactions.

Different ratios of IMO-11 with thiourea or sodium oleate hybrid inhibitors were loaded into the gel coating to enhance the self-healing ability. The SEM and FT-IR results confirmed the successfully prepared gel coating with a hybrid inhibitor. The inhibitors act in the dispersion phase of the gel coating which is loaded into the coating by physical dispersion and hydrogen bonding. The EIS and surface morphology observations revealed the great self-healing performance of scratched gel coatings. The release of the inhibitor could protect the steel at the scratch area by forming an adsorption film. In this study, the addition of an oil- or water-soluble inhibitor did not significantly alter the results.

Author Contributions: X.Z. (Xiong Zhao), Conceptualization, Data curation, and Writing—original draft. J.W., Methodology, Investigation, Data curation, and Writing—original draft. H.Z. (Haibing Zhang), Formal analysis and Investigation. H.Z. (Hailong Zhang), Formal analysis. L.M., Writing—review and editing. X.Z. (Xianfeng Zhang), Project administration. W.C., Formal analysis and Writing—review and editing. H.Z. (Huiyu Zhang), Formal analysis and Writing—review and editing. A.H.K., Writing—review and editing. B.L., Writing—review and editing, Supervision, and Funding Acquisition. J.T., Supervision and Funding Acquisition. All authors have read and agreed to the published version of the manuscript.

Funding: This research was supported by the National Natural Science Foundation of China (Grant No. 52201088), and the scientific research project of China Three Gorges Group Co., LTD (No. 202303051).

Institutional Review Board Statement: Not applicable.

Informed Consent Statement: Not applicable.

Data Availability Statement: Data are contained within the article.

Conflicts of Interest: Authors Xiong Zhao, Lu Ma, and Xianfeng Zhang were employed by the China Three Gorges Corporation company. The remaining authors declare that the research was conducted in the absence of any commercial or financial relationships that could be construed as a potential conflict of interest.

References

1. Zhang, F.; Ju, P.; Pan, M.; Zhang, D.; Huang, Y.; Li, G.; Li, X. Self-healing mechanisms in smart protective coatings: A review. *Corros. Sci.* **2018**, *144*, 74–88. [CrossRef]
2. Zhu, M.; Rong, M.Z.; Zhang, M.Q. Self-healing polymeric materials towards non-structural recovery of functional properties. *Polym. Int.* **2014**, *63*, 1741–1749. [CrossRef]
3. Peter, V.; Mats, M.; Yaiza, G.-G.; Herman, T.; Johannes, M.C.M. Electrochemical Evaluation of Corrosion Inhibiting Layers Formed in a Defect from Lithium-Leaching Organic Coatings. *J. Electrochem. Soc.* **2017**, *164*, C396. [CrossRef]
4. Attaei, M.; Calado, L.M.; Taryba, M.G.; Morozov, Y.; Shakoor, R.A.; Kahraman, R.; Marques, A.C.; Montemor, M.F. Autonomous self-healing in epoxy coatings provided by high efficiency isophorone diisocyanate (IPDI) microcapsules for protection of carbon steel. *Prog. Org. Coat.* **2020**, *139*, 105445. [CrossRef]
5. Toohey, K.S.; Hansen, C.J.; Lewis, J.A.; White, S.R.; Sottos, N.R. Delivery of Two-Part Self-Healing Chemistry via Microvascular Networks. *Adv. Funct. Mater.* **2009**, *19*, 1399–1405. [CrossRef]

6. Zhang, H.; Tang, J.; Han, H.; Zhang, S.; Wang, H.; Wang, Y.; Li, T.; Lin, B. Study on a Novel Recyclable Anticorrosion Gel Coating Based on Ethyl Cellulose and Thermoplastic Polyurethane. *Coatings* **2019**, *9*, 618. [CrossRef]
7. Zhang, H.; Li, S.; Zheng, H.; Han, Z.; Lin, B.; Wang, Y.; Guo, X.; Zhou, T.; Zhang, H.; Wu, J.; et al. A Visual Color Response Test Paper for the Detection of Hydrogen Sulfide Gas in the Air. *Molecules* **2023**, *28*, 5044. [CrossRef] [PubMed]
8. Zhang, H.; Lin, B.; Tang, J.; Wang, Y.; Wang, H.; Zhang, H.; Cao, J.; Hou, J.; Sun, M.; Zhang, H. An ethyl cellulose-based supramolecular gel composite coating for metal corrosion protection and its self-healing property from electromagnetic heating effect. *Surf. Coat. Technol.* **2021**, *424*, 127647. [CrossRef]
9. Wang, J.; Tang, J.; Zhang, H.; Wang, Y.; Wang, H.; Lin, B.; Hou, J.; Zhang, H. A CO_2-responsive anti-corrosion ethyl cellulose coating based on the pH-response mechanism. *Corros. Sci.* **2021**, *180*, 109194. [CrossRef]
10. Lin, B.; Wang, J.; Zhang, H.; Wang, Y.; Zhang, H.; Tang, J.; Hou, J.; Zhang, H.; Sun, M. Self-healing performance of ethyl-cellulose based supramolecular gel coating highly loaded with different carbon chain length imidazoline inhibitors in NaCl corrosion medium. *Corros. Sci.* **2022**, *197*, 110084. [CrossRef]
11. Fan, B.; Zhu, H.; Li, H.; Tian, H.; Yang, B. Penetration of imidazoline derivatives through deposited scale for inhibiting the under-deposit corrosion of pipeline steel. *Corros. Sci.* **2024**, *235*, 112209. [CrossRef]
12. Verma, C.; Quraishi, M.A.; Rhee, K.Y. Hydrophilicity and hydrophobicity consideration of organic surfactant compounds: Effect of alkyl chain length on corrosion protection. *Adv. Colloid Interface Sci.* **2022**, *306*, 102723. [CrossRef] [PubMed]
13. Zhu, Y.; Qu, S.; Shen, Y.; Liu, X.; Lai, L.; Dai, Z.; Liu, J. Investigation on the synergistic effects and mechanism of oleic imidazoline and mercaptoethanol corrosion inhibitors by experiment and molecular dynamic simulation. *J. Mol. Struct.* **2022**, *1274*, 134512. [CrossRef]
14. Wang, X.; Yang, J.; Chen, X.; Yan, K.; Wang, Y.; Yang, Z. Structure-Performance Relations of Thio-alcohols and their Synergistic Corrosion Inhibition for Carbon Steel in CO_2-saturated Solution. *J. Mol. Struct.* **2023**, *1299*, 137144. [CrossRef]
15. Ren, Y.; Zhang, J.; Du, M.; Niu, L. The synergistic inhibition effect between imidazoline-based dissymmetric bis-quaternary ammonium salts and thiourea on Q235 steel in CO_2 corrosion process. *Res. Chem. Intermed.* **2015**, *42*, 641–657. [CrossRef]
16. Okafor, P.C.; Liu, C.B.; Liu, X.; Zheng, Y.G.; Wang, F.; Liu, C.Y.; Wang, F. Corrosion inhibition and adsorption behavior of imidazoline salt on N80 carbon steel in CO_2-saturated solutions and its synergism with thiourea. *J. Solid State Electrochem.* **2010**, *14*, 1367–1376. [CrossRef]
17. Eivaz Mohammadloo, H.; Mirabedini, S.M.; Pezeshk-Fallah, H. Microencapsulation of quinoline and cerium based inhibitors for smart coating application: Anti-corrosion, morphology and adhesion study. *Prog. Org. Coat.* **2019**, *137*, 105339. [CrossRef]
18. Sanaei, Z.; Ramezanzadeh, B.; Shahrabi, T. Anti-corrosion performance of an epoxy ester coating filled with a new generation of hybrid green organic/inorganic inhibitive pigment; Electrochemical and surface characterizations. *Appl. Surf. Sci.* **2018**, *454*, 1–5. [CrossRef]
19. Saei, E.; Ramezanzadeh, B.; Amini, R.; Kalajahi, M.S. Effects of combined organic and inorganic corrosion inhibitors on the cerium based conversion coating performance on AZ31 Magnesium Alloy: Morphological and corrosion studies. *Corros. Sci.* **2017**, *127*, 186–200. [CrossRef]
20. *GB/T 5210*; Paints and varnishes—Pull-Off Test for Adhesion. China National Standardization Management Committee: Beijing, China, 2006.
21. Feng, Y.; Cheng, Y.F. An intelligent coating doped with inhibitor-encapsulated nanocontainers for corrosion protection of pipeline steel. *Chem. Eng. J.* **2017**, *315*, 537–551. [CrossRef]
22. Izadi, M.; Shahrabi, T.; Ramezanzadeh, B. Active corrosion protection performance of an epoxy coating applied on the mild steel modified with an eco-friendly sol-gel film impregnated with green corrosion inhibitor loaded nanocontainers. *Appl. Surf. Sci.* **2018**, *440*, 491–505. [CrossRef]
23. Li, L.; Dong, C.; Liu, L.; Li, J.; Xiao, K.; Zhang, D.; Li, X. Preparation and characterization of pH-controlled-release intelligent corrosion inhibitor. *Mater. Lett.* **2014**, *116*, 318–321. [CrossRef]
24. Haddadi, S.A.; Ramazani, S.A.A.; Mahdavian, M.; Arjmand, M. Epoxy nanocomposite coatings with enhanced dual active/barrier behavior containing graphene-based carbon hollow spheres as corrosion inhibitor nanoreservoirs. *Corros. Sci.* **2021**, *185*, 109428. [CrossRef]
25. Wen, J.; Lei, J.; Chen, J.; Gou, J.; Li, Y.; Li, L. An Intelligent Coating Based on pH-Sensitive Hybrid Hydrogel for Corrosion Protection of Mild Steel. *Chem. Eng. J.* **2019**, *392*, 123742. [CrossRef]
26. Shkrob, I.A.; Zhu, Y.; Marin, T.W.; Abraham, D. Reduction of Carbonate Electrolytes and the Formation of Solid-Electrolyte Interface (SEI) in Lithium-Ion Batteries. 1. Spectroscopic Observations of Radical Intermediates Generated in One-Electron Reduction of Carbonates. *J. Phys. Chem. C* **2013**, *117*, 19255–19269. [CrossRef]
27. Zhao, D.; Liu, S.; Wu, Y.; Guan, T.; Sun, N.; Ren, B. Self-healing UV light-curable resins containing disulfide group: Synthesis and application in UV coatings. *Prog. Org. Coat.* **2019**, *133*, 289–298. [CrossRef]
28. Attia, A.M.A.; Nour, M.; El-Seesy, A.I.; Nada, S.A. The effect of castor oil methyl ester blending ratio on the environmental and the combustion characteristics of diesel engine under standard testing conditions. *Sustain. Energy Technol. Assess.* **2020**, *42*, 100843. [CrossRef]
29. Aayisha, S.; Renuga Devi, T.S.; Janani, S.; Muthu, S.; Raja, M.; Sevvanthi, S. DFT, molecular docking and experimental FT-IR, FT-Raman, NMR inquisitions on "4-chloro-N-(4,5-dihydro-1H-imidazol-2-yl)-6-methoxy-2-methylpyrimidin-5-amine": Alpha-2-imidazoline receptor agonist antihypertensive agent. *J. Mol. Struct.* **2019**, *1186*, 468–481. [CrossRef]

30. Martín-Alfonso, J.E.; Martín-Alfonso, M.J.; Franco, J.M. Tunable rheological-tribological performance of "green" gel-like dispersions based on sepiolite and castor oil for lubricant applications. *Appl. Clay Sci.* **2020**, *192*, 105632. [CrossRef]
31. Mahmoud, S.; Mohammad Hossein, A.; Alireza Sabour, R. Synergistic Corrosion Inhibition of Benzotriazole and Thiourea for Refineries and Petrochemical Plants. *Prot. Met. Phys. Chem. Surf.* **2022**, *58*, 200–215. [CrossRef]
32. Liu, W.; Zhang, J.; Wang, W.; Deng, J.; Chen, B.; Yan, W.; Xiong, S.; Huang, Y.; Liu, J. Flotation behaviors of ilmenite, titanaugite, and forsterite using sodium oleate ads the collector. *Miner. Eng.* **2015**, *72*, 1–9. [CrossRef]
33. Maia, F.; Tedim, J.; Lisenkov, A.D.; Salak, A.N.; Zheludkevich, M.L.; Ferreira, M.G.S. Silica nanocontainers for active corrosion protection. *Nanoscale* **2012**, *4*, 1287–1298. [CrossRef] [PubMed]
34. Huang, Y.; Zhao, C.; Li, Y.; Wang, C.; Shen, T.; Wu, C.; Hu, Z.; Cheng, D.; Yang, H. Enhanced corrosion resistance and self-healing effect of sol–gel coating incorporating one-pot-synthesized corrosion inhibitor encapsulated silica nanocontainers. *J. Sol Gel Sci. Technol.* **2022**, *104*, 78–90. [CrossRef]
35. Jiang, J.; Tang, Y.; Huang, L.; Peng, L.; Xu, Y.; Wei, G.; Li, Y. Nano-emulsification method as a strategy for oil soluble corrosion inhibitor transform to water soluble. *J. Mol. Liq.* **2023**, *386*, 122420. [CrossRef]
36. Fan, W.; Li, W.; Zhang, Y.; Wang, W.; Zhang, X.; Song, L.; Liu, X. Cooperative self-healing performance of shape memory polyurethane and Alodine-containing microcapsules. *RSC Adv.* **2017**, *7*, 46778–46787. [CrossRef]